JOURNAL OF APPLIED ELECTROCHEMISTRY 25 (1995) 347–352

Improved corrosion resistance of pulse plated nickel through crystallisation control

P. T. TANG*, T. WATANABE†, J. E. T. ANDERSEN*, G. BECH-NIELSEN§

*Centre of Advanced Electroplating (CAG), The Technical University of Denmark, Building 425, 2800 Lyngby, Denmark

†Department of Industrial Chemistry, Tokyo Metropolitan University, 1-1 Minami-osawa, Hachioji-shi, Tokyo 192-03, Japan

§Chemistry Department A., The Technical University of Denmark, Building 207, 2800 Lyngby, Denmark

Received 18 May 1994; revised 16 September 1994

When electrodeposition of nickel is used for corrosion protection of steel two aspects are important: the porosity of the coating and the resistance against corrosion provided by the coating itself. Using simple pulsed current (PC) plating, the size of the deposited crystals can be significantly smaller, thereby reducing porosity correspondingly. This usually also leads to improved hardness of the coating. Introducing pulse reversal (PR) plating, the most active crystals are continuously dissolved during the anodic pulse, providing a coating with improved subsequent corrosion resistance in almost any corrosive environment. This correlation between film texture and corrosion resistance will be discussed.

1. Introduction

The effect of pulse plating on electrodeposition of nickel has been described in several studies. Grain size refinement as a result of relative high frequency (>10 Hz) pulsed current (PC) has been reported by Paatsch [1] and others [2, 3]. Fewer results have been reported on pulse reversal (PR) plating of nickel [3, 4].

A correlation between the crystal orientation planes and the corrosion potential during anodic polarization has been reported [5]. Others have studied the growth of nickel crystals on different substrates as a result of pulse plating parameters [6]. In this investigation, however, we concentrate on steel substrates and production applicable frequencies and equipment.

The deposition of nickel takes place through a number of intermediate steps ([7], among several others) as indicated below:

$$Ni^{2+} + H_2O \longleftrightarrow NiOH^+ + H^+$$

$$NiOH^+ + e^- \longrightarrow NiOH_{ad}$$

$$NiOH_{ad} + H^+ + e^- \longleftrightarrow Ni^0 + H_2O$$

Pulsed current (PC) plating with short cathodic pulses (1 ms or less) and high current densities (approximately 16 A dm^{-2} or more) give rise to another deposition mechanism [8].

Based on a significant increase in pH near the cathode surface during a pulse, a layer of colloidal nickel hydroxide is formed:

$$Ni^{2+} + 2OH^- \longrightarrow [Ni(OH)_2]_{colloidal}$$

From this layer micelles are formed by attaching additional nickel ions:

$$\{Ni^{2+}[Ni(OH)_2]\}_{colloidal}$$

Nickel deposition from this layer has a semibright appearance, and a clearly different texture (Figs 6 and 8) as compared to DC-plated nickel.

Nickel plating for the protection of steel against corrosion is an extensively used process. Using pulse reversal plating it is possible to improve material distribution [9] (throwing power) and at the same time obtain more resistant coatings. A specified level of corrosion protection can then be met with a lower amount of nickel deposited. This aspect has environmental as well as economic advantages.

2. Experimental details

All the nickel electrolytes used in this investigation were based on the Watts solution. Numerous versions of this bath exist, but the concentrations usually are [10]: nickel sulphate 240–300 g dm^{-3}, nickel chloride 40–60 g dm^{-3} and boric acid 25–40 g dm^{-3}.

The amount of nickel chloride affects mechanical properties such as internal stress and hardness. A Watts electrolyte with a high chloride content produces harder coatings with substantial (tensile) stress [10]. The amount of chloride in a Watts electrolyte also determines the solubility of the anodes (pure nickel). Low concentrations of chloride decrease the current efficiency and make PR impossible due to passivation of the surface during anodic pulses.

A typical Watts bath, referred to as W2, was

0021-891X

Table 1. Composition of a typical Watts nickel bath (W2) and the alternative bath (W3) used for the electrochemical studies

	W2	*W3*
Nickel sulphate $NiSO_4 . 6H_2O$ g dm^{-3}	300	250
Nickel chloride $NiCl_2 . 6H_2O$ g dm^{-3}	50	100
Boric acid H_3BO_3 g dm^{-3}	40	40
pH	4.5	4.0

Table 2. Pulse plating patterns applied to samples for corrosion and X-ray diffraction experiments

Pattern	I_c/A dm^{-2}	T_c/ms	I_a/A dm^{-2}	T_a/ms
DC	3.45	–	–	–
PC1	3.45	80	0	20
PC2	17.24	1	0	19
PR	3.45	40	8.63	10

compared to a Watts bath in which some of the nickel sulphate had been substituted by nickel chloride (Table 1). Electrochemical studies of these two baths lead to several interesting results. Both of the two experiments illustrated in Fig. 1, were carried out at 50°C using a rotating disc electrode (1000 rpm). After a suitable cathodic period at 2 A dm^{-2}, a potential sweep from approximately −600 mV vs SHE to 200 mV at 2 mV s^{-1} was conducted.

Studying the cathodic parts of the two curves, both baths appear to have a limiting current for the reduction of H^+ ions at approximately 0.02–0.03 A dm^{-2}. Moving further in the cathodic direction (from approximately −350 to −600 mV) this limiting current region is followed by a stable section which is expected to continue until the limiting current for the reduction of nickel ions is approached. The anodic curves are the most interesting parts for this investigation, because of the significant difference in the value for maximum anodic current density before passivation occurs. The extra concentration of chloride (and smaller concentration of sulphate) in the W3 electrolyte clearly enables a faster dissolution of the already deposited nickel, which is required for the desired effects of pulse reversal plating. For this reason it was decided, after the electrochemical investigation, to use the W3 bath only at a temperature of 53° C ± 1° C, a pH of 4.2 ± 0.1 and a bath volume of 65 litres. This bath was used with air agitation and mild steel or stainless steel substrates (75 mm × 75 mm × 1 mm, total plateable area = 1.16 dm^2). For the acid dip corrosion tests stainless steel substrates were used, activated by a short period (20 s) with anodic potential (3 V) and a longer cathodic period (60 s, 2 V) in a Wood nickel bath (100 g dm^{-3} $NiCl_2 . 6H_2O$ and 100 cm^3 dm^{-3} concentrated hydrochloric acid). For the X-ray diffraction investigations, the deposited nickel films were removed from the stainless steel substrate (the substrates were not activated) to avoid false reflections. For all other experiments mild steel substrates were used.

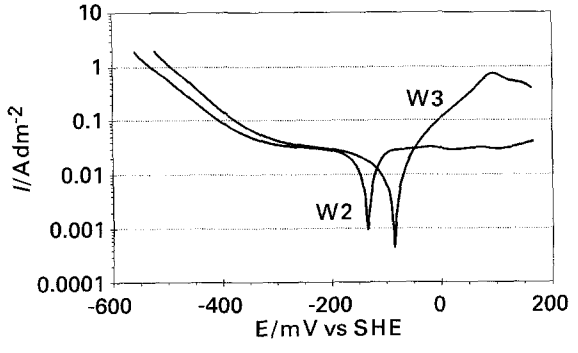

Fig. 1. Potential sweeps showing the maximum anodic current density before passivation occurs. For W2 and W3 see text.

2.1. *Pulse plating*

Four different pulse patterns were selected for various reasons. Two types of pulsed current, one known to reduce porosity [1, 9] (PC1) and one following the deposition model proposed by Kostin *et al.* [8] (PC2). A single pulse reversal (PR) pattern was selected in order to study the texture of this type of deposits. This specific pulse reversal pattern is known to improve the distribution of material [9], since the nickel plated onto high current density areas of the substrate during cathodic potentials is dissolved during the anodic pulses. It is important that the anodic current density is significantly higher than the cathodic current density. Finally a direct current (DC) pattern was used for comparison. The current density for DC was the same as the cathodic current density in PC1 and PR (Table 2).

Using pulse plating the time needed to deposit a given amount of nickel is usually increased, but if the quality of the coating is improved and the material more evenly distributed, the time needed to meet a certain specification may be the same.

All experiments started with a ramp, for example, a continuously increased current density from 0 to 3.45 A dm^{-2} in 60 s. This procedure ensures that the substrate is covered with nickel before the actual pulse plating begins.

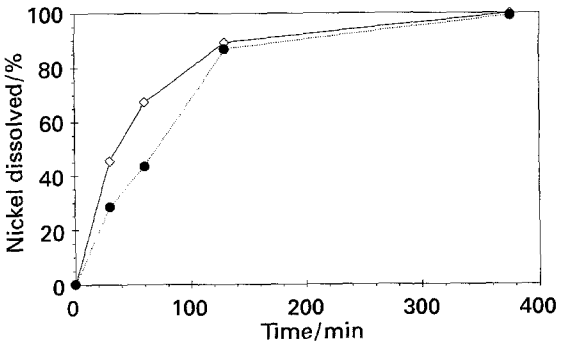

Fig. 2. Nickel dissolution measured by weight loss in percentage of initial weight. Samples submerged in 7 M nitric acid. Key: (◇) DC; (●) PR.

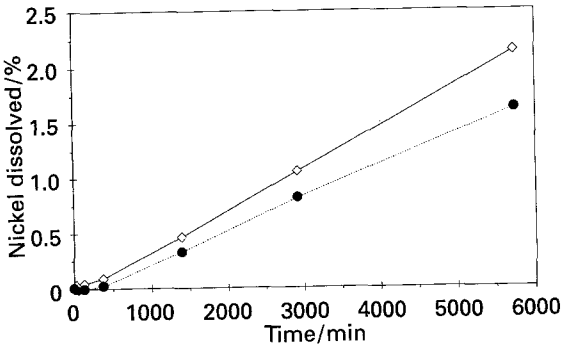

Fig. 3. Corrosion performance of (●) pulse reversal (PR) and (◇) direct current (DC) plated nickel deposits in a 20 g dm^{-3} citric acid solution.

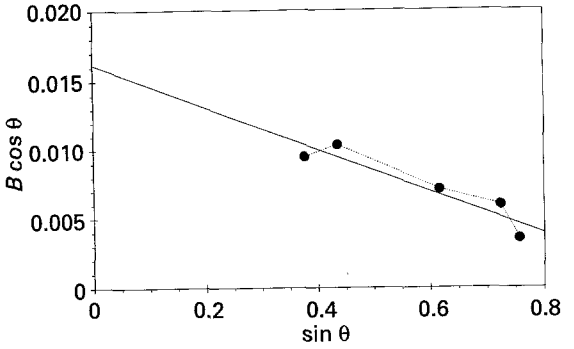

Fig. 5. Fit of straight line to the data for the DC sample, according to Equation 1. The dotted line connecting the data points is shown for clarity only. All angles are in radians.

All pulse plating was carried out using the computer aided pulse plating (CAPP) [11] system developed by the Centre of Advanced Electroplating (CAG). The system consists of a rectifier (12 V, 20 A) and an interface to a computer performing precise programming and execution of pulse patterns.

3. Results

Nickel deposition was performed by passing a total charge of 7800 C to each panel (corresponding to a nickel coating thickness of approximately 12 μm), regardless of the pulse pattern or test method used.

3.1. *Corrosion tests*

Using different acid solutions, the dissolution of PR and DC plated nickel (Table 2) were measured as the weight loss (percentage of initial deposit weight) as a function of time (minutes in acid solution). In these experiments stainless steel was used as the substrate in order to avoid interference from dissolved substrate elements.

After 30 min in 7 M nitric acid, 25% of the PR deposit had been dissolved while almost 50% of the DC deposit had been dissolved. After 60 min the nickel coating was completely stripped off a circular area in the middle on both sides of the DC panel, while the PR panel was still free of perforations (also due to the improved distribution of metal caused by this pulse pattern [9]). Eventually, after 375 min, all nickel on both panels had been dissolved (Fig. 2). Similar experiments using a 20 g dm^{-3} citric acid solution (Fig. 3) and 3 M hydrochloric acid, showed that the pulse reversal plated nickel corroded significantly slower than the conventional DC deposits.

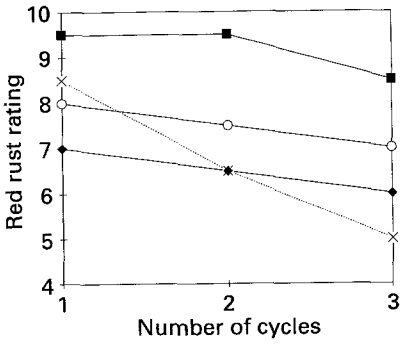

Fig. 4. Result of the moist SO_2-test. A rating of 10 means no visible red rust. Key: (○) DC, (×) PC1, (◆) PC2 and (■) PR.

In each of these acid dip experiments, the weight of the stainless steel substrates was measured before activation and nickel plating, and again after the nickel coating had been completely dissolved. In all cases, the weight loss of the substrate was insignificant.

A very efficient corrosion test for nickel plated mild steel substrates, is the moist SO_2-test (ASTM G 87-84). Two panels of each of the four pulse patterns were plated with nickel from the W3 bath. The panels were then exposed in the chamber for 8 h at 40° C with 0.2 litres of SO_2 gas. They were then washed, dried and evaluated according to ASTM B 537-70, and made ready for another cycle. The test determines the efficiency of corrosion protection provided by the nickel coating. It is not possible with this test to distinguish between low porosity and low dissolution rate of the coating itself (Fig. 4).

3.2. *X-ray diffraction*

The films were analysed by X-ray diffraction with a Rigaku RAD-IC instrument using Cu$K\alpha$ radiation. The angle between the incident X-ray beam and the face of the films was changed from 40.00° up to 110.00° to measure the diffraction patterns.

The X-ray diffraction patterns of the four films (Figs. 6–9) are characterised with respect to texture [$h\,k\,l$], effective size of crystallites (D_e) and root mean square non uniform strain ($\bar{\epsilon}$) by standard methods [12, 13]. By assuming that the diffraction lines approximate Cauchy profiles, the integral breadth (B) corrected for instrumental broadening is expressed by

$$B = \frac{\lambda}{D_e \cos\theta} + 2\bar{\epsilon}\tan\theta \qquad (1)$$

in which θ is the diffraction angle and λ the X-ray wavelength. The integral breadth B (in radians) is

Table 3. Effective size of crystallites (D_e) and root mean square non uniform strain ($\bar{\epsilon}$) obtained by straight line analysis of the diffraction lines

All diffraction lines applied	*DC*	*PC1*	*PC2*	*PR*
D_e/nm	9.5 ± 1.2	5.0 ± 1.0	9.4 ± 4.5	9.5 ± 2.0
$\bar{\epsilon}$	-0.008 ± 0.002	-0.015 ± 0.006	-0.006 ± 0.007	-0.007 ± 0.003
Only the (1 1 1) and (2 2 2) lines applied	*DC*	*PC1*	*PC2*	*PR*
D_e/nm	9.9	4.3	10.3	9.9
$\bar{\epsilon}$	−0.008	−0.021	−0.008	−0.007

calculated from the diffraction line half-width (B′):

$$B = \frac{\pi B'}{2} = \frac{\pi^2}{360}\Delta B \qquad (2)$$

in which ΔB is the diffraction line half-width measured in degrees. By plotting $B\cos\theta$ against $\sin\theta$ values of D_e in the $[h\,k\,l]$ direction and of $\bar{\epsilon}$ can be obtained from Equation 1.

Figure 5 displays the results of such a calculation. In the analysis five diffraction lines with different directions $[h\,k\,l]$ of each experiment are applied. Within the uncertainty on the slopes and intercepts of the straight lines this procedure yielded slopes and intercepts which were not different from the analysis carried out by lines from a single direction (Table 3). For all four films the straight lines obtained had negative slopes.

For the films DC, PC1 and PR the straight line analysis fitted the data well, but for the film PC2 the deviations of the data from a straight line were rather large. The reason for this large deviation may be related to other effects causing line broadening and line asymmetry [12, 13]. The PC1 film had smaller effective crystallites and numerically larger values of $\bar{\epsilon}$ compared to the other films. Among the films DC, PC2 and PR no significant differences in values of D_e and of $\bar{\epsilon}$ were revealed by the straight line analysis ($D_e = 9.5$ nm and $\bar{\epsilon} = -0.007$).

An analysis of the film textures can be found in Table 4, where the intensities are given in percentages of the (1 1 1) line intensity. For comparison the intensity ratios of the ASTM powder analysis [14] is shown.

The PC1 film has intensity ratios which compare well with the powder analysis. This implies that the crystallites in the PC1 film are randomly oriented and thus the film has no specific texture. The intensities of the films DC, PC2 and PR reveal significant texture as compared to the powder analysis. For the DC film the (2 2 0) line is dominating, for the PC2 film the (2 2 0) line is even more dominating and for the PR film the (2 0 0) line dominates. By comparing the results of Table 3 with those of Table 4 little or no correlation between the effective size of crystallites and film texture is seen.

Table 4. Texture in the nickel films
The intensities are normalised to the intensity of the (1 1 1) diffraction line

Reflection	*Powder [14]*	*DC*	*PC1*	*PC2*	*PR*
(1 1 1)	100	100	100	100	100
(2 0 0)	42	33	35	20	72
(2 2 0)	21	53	24	235	4
(3 1 1)	20	21	31	25	24
(2 2 2)	7	5	7	5	4

4. Discussion

The difference in film texture, as observed with X-ray diffraction, cannot be directly compared by inspecting Table 4. Although the conditions for obtaining the X-ray diffraction result were the same for all samples (Figs 6–9) the total intensity for each film shows considerable variation, predominantly due to differences in the film thickness. Although each sample was prepared in the same way and by passing the same number of coulombs, there are still differences in thickness because of variations in current efficiency, deposition mechanism and local and global current densities. To emphasize the differences between the investigated pulse patterns, as far as texture is concerned, a comparison of absolute intensities has been carried out as shown in Table 5. By adding the intensities of the five most dominating diffraction lines (Table 4) all intensities are normalized to the corresponding intensities for PC1, which is the film that compares well to the powder analysis in which all orientations are equally represented. The observations of film texture are not altered by this normalization, but the relative changes are better quantified.

Thus, the number of crystallites with (2 2 0) orientation has doubled in DC compared to PC1 while the number of (2 2 0) orientated crystallites in PC2 is five times more than for PC1. For PR (2 2 0) is almost extinguished while (2 0 0) reflection is increased (Table 5).

Considering the comparative investigation of the dissolution of DC and PR plated nickel in different acid solutions, such as nitric or citric acid, which showed a small but consistent difference, a likely explanation is that the corrosion rate for (2 2 0) crystallites (preferred orientation for DC) is generally higher than the corrosion rate of (2 0 0), which is the preferred orientation of PR.

Comparing all four types of pulse plated nickel using the moist SO_2-test, the results are seen as a

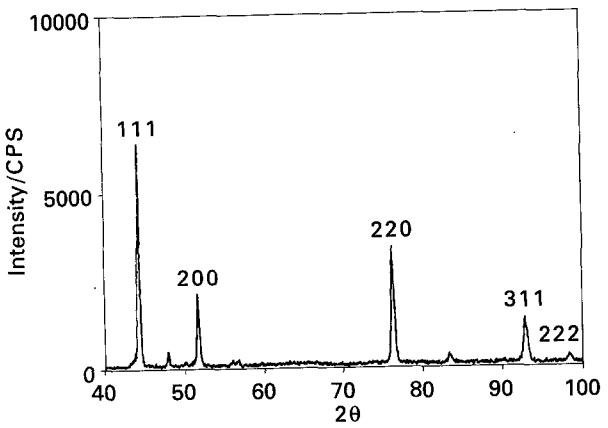

Fig. 6. X-ray diffraction results for the DC nickel film. Intensity (CPS) against 2θ measured in degrees.

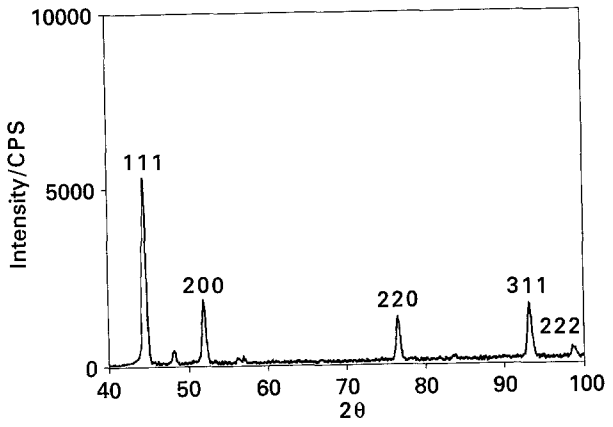

Fig. 7. X-ray diffraction diagram for PC1. The pattern is comparable to the distribution of powder nickel [14].

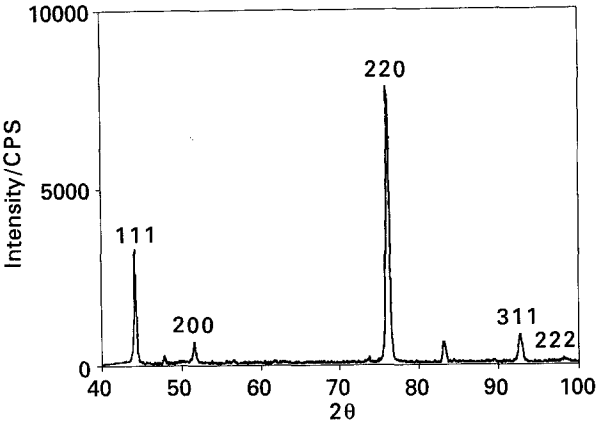

Fig. 8. X-ray diffraction results for the PC2 nickel film. Note the relatively high intensity of the (2 2 0) reflection.

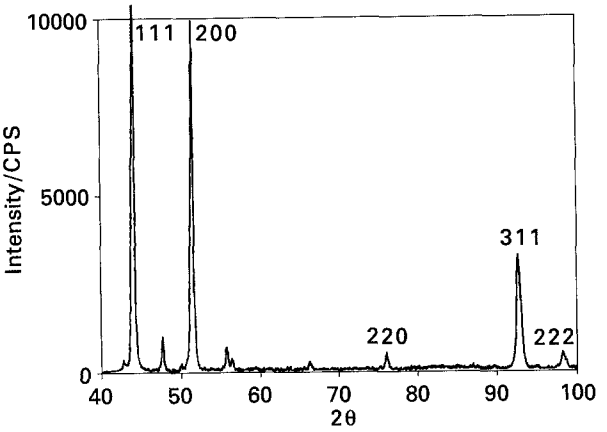

Fig. 9. X-ray diffraction for PR. The intensity of (2 2 0) is almost extinguished while the intensity of (2 0 0) is profound.

combination of porosity and corrosion resistance. This makes it more difficult to determine which crystal orientation is responsible for a specific result, but some indications should be emphasised: As mentioned above, the PR plated samples are significantly better than DC, partly because of the improved material distribution achieved through pulse reversal plating [9] and partly due to the shift in preferred crystal orientation from (2 2 0) to (2 0 0).

Using pulsed current (PC1 and PC2) does not seem to improve corrosion resistance in any way. PC1 has, possibly because of reduced grain size, relatively high rating after the first cycle in the moist SO_2-test, but a lower rating later because of rapid corrosion of the nickel film itself. PC2 is inferior to DC, which again indicates that crystallites of the (2 2 0) orientation are not as resistant as crystallites with (2 0 0) or (1 1 1) orientation.

Table 5. Film texture comparison
Values in percentage of the corresponding line of PC1

Reflection	*DC*	*PC1*	*PC2*	*PR*
(1 1 1)	93	100	51	93
(2 0 0)	89	100	30	203
(2 2 0)	201	100	493	14
(3 1 1)	64	100	42	75
(2 2 2)	61	100	32	48

5. Summary

Electrodeposition of nickel using pulse plating techniques can provide coatings with improved corrosion resistance as compared with DC plating. With pulse reversal plating it is furthermore possible to reduce the corrosion rate of the nickel coating itself in various environments. The reason for this improved corrosion resistance is found in the distinct changes in texture as determined by X-ray diffraction studies. The X-ray diffraction lines follow a Cauchy profile and the rootmean non uniform strain is −0.007.

References

[1] W. Paatsch, *Metalloberfläche* **40** (1986) 387–390.
[2] W. Kleinekathöfer, Ch. J. Raub and E. Raub, *ibid.* **9** (1982) 411–420.
[3] J-Cl. Puippe (ed.), 'Theory and Practice of Pulse Plating', American Electroplaters and Surface Finishers Society (AESF), Orlando (1986).
[4] T. P. Sun, C. C. Wan and Y. M. Shy, *Metal Finish.* **5** (1979) 33–38.
[5] I. Garz, H. Worch and W. Schatt, *Corros. Sci.* **9** (1969) 71.
[6] C. Kollia, N. Spyrellis, J. Amblard, M. Fromant and G. Maurin, *J. Appl. Electrochem.* **20** (1990) 1025–1032.
[7] A. J. Bard (ed.), 'Encyclopaedia of the Electrochemistry

of the Elements', Marcel Dekker, New York (1982) Chapter III–3.
[8] N. A. Kostin, A. K. Krivtsov, V. S. Abdulin and V. A. Zabludovskii, *Élektrokhimiya* **18** (1982) 210–214.
[9] P. T. Tang, P. Leisner and P. Møller, 'Improvement of Nickel Deposit Characteristics by Pulse Plating' SUR/FIN '93, Anaheim, 21–24 June (1993).
[10] S. A. Watson, 'Compendium on Nickel Electroplating and Electroforming', Nickel Development Institute, Technical reports 10047–10055 (1989).
[11] T. C. Dörge, P. Møller and P. Leisner, 'Design of Potentiostatic/Galvanostatic Waveforms for Pulse Plating Control: Features and Applications', AESF Pulse Plating Symposium, Orlando (1991).
[12] H. P. Klug and L. P. Alexander, 'X-ray Diffraction Procedures', John Wiley & Sons, New York (1974).
[13] R. W. Vook and F. Witt, *J. Vac. Sci. Technol.* **2** (1965) 49.
[14] American Society for Testing Materials, X-ray Department, Philadelphia, PA.